

Preparation of Disilanobithiophene-benzothiadiazole Polymer for High-voltage Bulk Heterojunction-type Polymer Solar Cell

Joji Ohshita,^{*, †} Makoto Nakashima,[†] Daiki Tanaka,[†] Yasushi Morihara,[‡] Hiroyuki Fueno,[§] Kazuyoshi Tanaka[§]

[†]Department of Applied Chemistry, Graduate School of Engineering, Hiroshima University, Higashi-Hiroshima 739-8527, Japan

[‡]Synthesis Research Laboratory, Kurashiki Research Center, Kuraray Co., Ltd., 2045-1 Sakazu, Kurashiki 710-0801, Japan

[§]Division of Molecular Engineering, Graduate School of Engineering, Kyoto University, Nishikyo-Ku Kyoto 615-8510, Japan

Supporting Information

Experimental

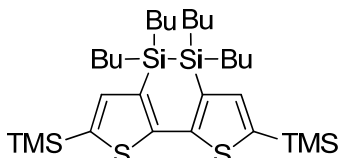
General. All reactions were carried out under a dry argon atmosphere. THF, ether, and toluene used as the reaction solvents were distilled from calcium hydride and were stored over activated molecular sieves before use. The starting reagents, 3,3'-dibromo-5,5'-bis(trimethylsilyl)-2,2'-bithiophene^a and 1,1,2,2-tetrabutyl-1,2-dichlorodisilane^b were prepared according to the procedure reported in the literature. NMR spectra were measured on Varian 400-MR and Varian System500 spectrometers. EI-mass spectra were obtained on a Shimadzu QP5050A spectrometer. UV-vis absorption spectra were measured on a SHIMADZU-UV-3150 spectrometer. GPC was carried out using serially connected Shodex KF2001 and KF2002 columns and THF as the eluent. Fabrication of PCSSs was performed as reported in the literature.^c

^a Ohshita, J.; Nodono, M.; Kai, H.; Watanabe, T.; Kunai, A.; Komaguchi, K.; Shiotani, M.; Adachi, A.; Okita, K.; Harima, Y.; Yamashita, K.; Ishikawa, M. *Organometallics* **1999**, *18*, 1453.

^b Iwahara, T.; Hayase, S.; West, R. *Macromolecules* **1990**, *23*, 1300.

^c Ohshita, J.; Miyazaki, M.; Zhang, F.-B.; Tanaka, D.; Morihara, Y. *Polymer J.* **2013**, in press (doi:10.1038/pj2013.13).

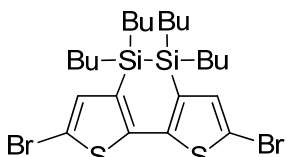
Preparation of DSBTSi



DSBTSi

To a solution of 7.03 g (15.0 mmol) of 3,3'-dibromo-5,5'-bis(trimethylsilyl)-2,2'-bithiophene in 150 mL of THF was added 18.0 mL (30.0 mmol) a 1.67 M *n*BuLi solution in hexane at -80°C. After stirring the resulting mixture at this temperature for 1.5 h, 5.34 g (15.0 mmol) of 1,1,2,2-tetrabutyl-1,2-dichlorodisilane was added to the mixture and the mixture then further stirred at room temperature for 10 h. The mixture was hydrolyzed with water and the organic layer was separated. The aqueous layer was extracted with hexane. The organic layer and the extracts were combined and dried over anhydrous magnesium sulfate. After evaporation of the solvents, the residue was subjected to silica gel chromatography eluting with hexane to give 4.64 g (7.82 mmol, 52% yield) of **DSBTSi** as light yellow viscous oil: EI-MS: *m/z* = 592 [M⁺]; ¹H NMR (δ in CHCl₃) 0.33 (s, 18H, MeSi), 0.77-0.94 (m, 20H, *n*Bu), 1.26-1.37 (m, 16H, *n*Bu), 7.13 (s, 2H, thiophene); ¹³C NMR (δ in CHCl₃) δ 0.05, 12.50, 13.70, 26.60, 27.05, 133.77, 138.05, 140.32, 150.92.

Preparation of DSBTBr

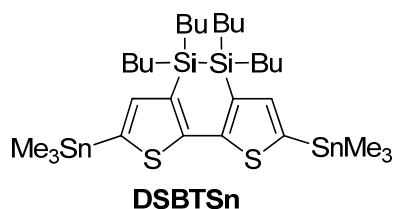


DSBTBr

To a solution of 4.27 g (7.20 mmol) of **DSBTSi** in 72 mL of chloroform was added 2.56 g (14.4 mmol) of *N*-bromosuccinimide (NBS) in a few portions at 0°C and the resulting mixture was stirred for 1 h. The mixture was hydrolyzed with water and the organic layer was washed with sodium thiosulfate (aq) then with water. The organic layer was dried over anhydrous magnesium sulfate. After evaporation of the solvents, the residue was subjected to silica gel chromatography eluting with hexane to give 4.02 g (6.63 mmol, 79% yield) of **DSBTBr** as yellow viscous oil: EI-MS *m/z* 606 [M⁺]; ¹H NMR (δ in CHCl₃) 0.75-0.92 (m, 20H, *n*Bu), 1.25-1.34 (m, 16H, *n*Bu), 6.95 (s, 2H, thiophene); ¹³C NMR (δ in CHCl₃) 12.31, 13.62, 26.55, 26.92, 110.11, 134.65, 135.64,

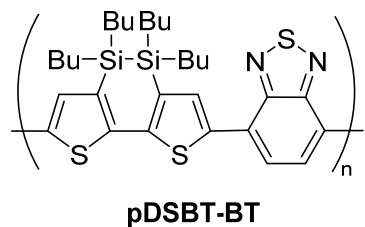
145.98. Anal Calcd for $C_{24}H_{38}Br_2S_2Si_2$: C, 47.51; H, 6.31. Found: C, 47.68; H, 6.23.

Preparation of **DSBTSn**



To a solution of 1.23 g (2.03 mmol) of **DSBTBr** in 20 mL of ether was added drop wise 2.44 mL (4.00 mmol) of a 1.67 M *n*BuLi solution in hexane at -80°C. After stirring the mixture for 1 h, 0.877 g (4.40 mmol) of trimethyltin chloride was added. The resulting mixture was allowed to warm to room temperature and stirred overnight. After hydrolysis with ice-water, the organic layer was separated and the aqueous layer was extracted with hexane. The organic layer and the extracts were combined and dried over anhydrous magnesium sulfate. After evaporation, the residue was subjected to preparative GPC eluting with toluene to give 1.08 g (1.39 mmol, 68% yield) of **DSBTSn** as dark green viscous oil: EI-MS *m/z* 776 [M⁺]; ¹H NMR (δ in $CHCl_3$) 0.37 (s, 18H, MeSn), 0.78-0.95 (m, 20H, Bu), 1.29-1.35 (m, 16H, Bu), 7.09 (s, 2H, thiophene); ¹³C NMR (in $CHCl_3$) δ -8.09, 12.60, 13.70, 26.63, 27.08, 132.89, 135.28, 141.33, 151.64. Anal Calcd for $C_{30}H_{56}S_2Sn_2$: C, 46.52; H, 7.29. Found: C, 46.75; H, 7.44.

Preparation of pDSBT-BT



pDSBT-BT

A mixture of 0.200 g (0.258 mmol) of **DSBTSn**, 7.59×10^{-2} g (0.258 mmol) of 4,7-dibromo-2,1,3-benzothiadiazole, 1.18×10^{-2} g (1.29×10^{-2} mmol) of $Pd_2(dba)_3$, 1.59×10^{-2} g (5.16×10^{-2} mmol) of (*o*-tolyl)₃P, and 15 mL of toluene was stirred at 70°C for 3 days. The resulting mixture was allowed to cool down to room temperature and a 30 mL aqueous solution of sodium N,N-diethyldithiocarbamate trihydrate (3.1 g) was added and the mixture was heated to 80°C for 2 hours. The organic layer was separated and washed with, in order, water, 3 vol% acetic acid aqueous solution, and

then water again. The organic layer was dried over anhydrous magnesium sulfate and the solvent was removed under vacuum. The residue was reprecipitated in the following order: from toluene/methanol, toluene/ethanol, and toluene/ethyl acetate, to provide 73.0 mg (49% yield) of **pDSBT-BT** as red-purple solids: mp >300°C; ¹H NMR (δ in C₆D₅Cl) 0.97-2.00 (br m, 40H, Bu), 7.20-7.71 (br m, 2H, thiophene), 8.50 (br s, 2H, benzothiaziazole); ¹³C NMR (δ in C₆D₅Cl) 13.21, 14.01, 27.10, 27.66, aromatic carbon signals could not be observed likely due to the signal broadening; GPC M_n = 20,000, M_w = 39,000, M_w/M_n = 1.9; UV-Vis abs λ_{max} = 633 nm (in THF).

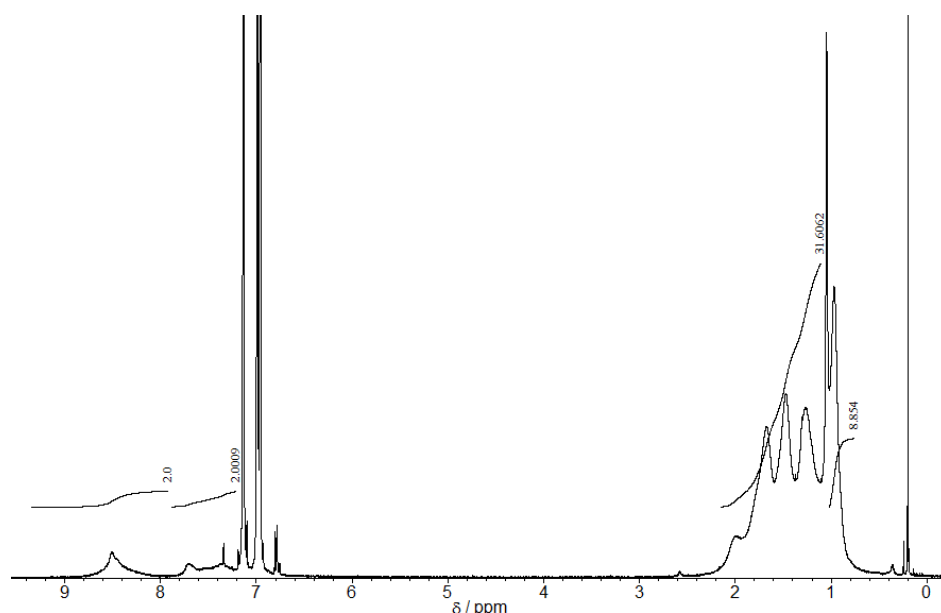


Figure S-1. ¹H NMR spectra of **pDSBT-BT** in C₆D₅Cl.

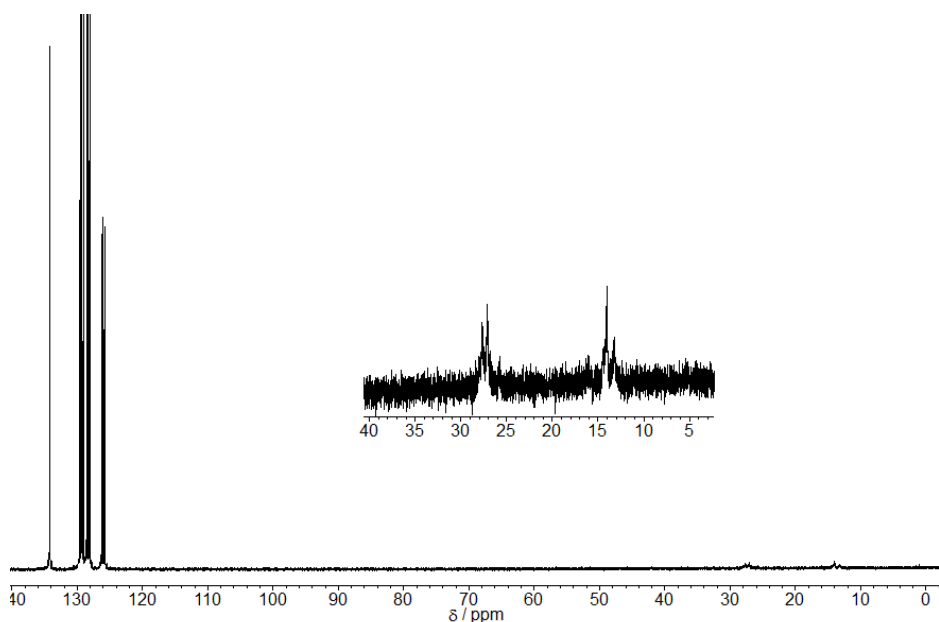


Figure S-2. ¹³C NMR spectra of **pDSBT-BT** in C₆D₅Cl.

Theoretical Calculation of the Modeled Polymers

The geometry optimizations of modeled polymers **pDSBT-BT** and **pDTS-BT** were performed based on the one-dimensional crystal orbital (CO) calculations at the B3LYP/6-31G(d,p) level using Gaussian 09 program package.^d The HOCO and the LUCO patterns and Mulliken analysis values are obtained by the B3LYP/STO-6G calculations using the Crystal 09 program package^e for the above optimized polymer structures due to a characteristic feature of Gaussian 09.

The optimized structures represented by the unit cells and selected structural parameters of **pDSBT-BT** and **pDTS-BT** are shown in Figures S-3 – S-6. It is seen in Figs. S-3 and S-4 that the energetically more stable structures of both **pDSBT-BT** and **pDTS-BT** have bithiophene and thiadiazole rings in somewhat similar side although coplanarity between these two rings is not reserved more or less as seen in Figures S-5 and S-6. The dihedral angle values between the bithiophene and the phenyl rings of these two polymers in Figures S-5 and S-6 definitely show the non-planar structures of them and that **pDSBT-BT** is more twisted. On the other hand, the HOCO and the LUCO patterns in Figures S-7 and S-8 show that π -characteristic features are not so much damaged in spite of the mentioned twisted structures perhaps due to somewhat flexibility of the π -conjugation even for the distorted co-planarity as often seen in C₆₀ or

carbon nanotubes. Results of the series of Mulliken analyses are depicted in Figures S-9 – S-12. The cationic property of Si atom is the larger in **pDTS-BT** (+0.845) than those in **pDSBT-BT** (+0.631 and +0.632) but those of S atoms are almost similar in these two polymers.

^d Gaussian 09, Rev. C.01, Frisch, M. J. et al., Gaussian Inc., Wallingford CT, 2010.

^e Dovesi, R.; Orlando, R.; Civalleri, B.; Roetti, C.; Saunders, V. R.; Zicovich-Wilson, C. *M. Z. Kristallogr.* **2005**, *220*, 571-573.

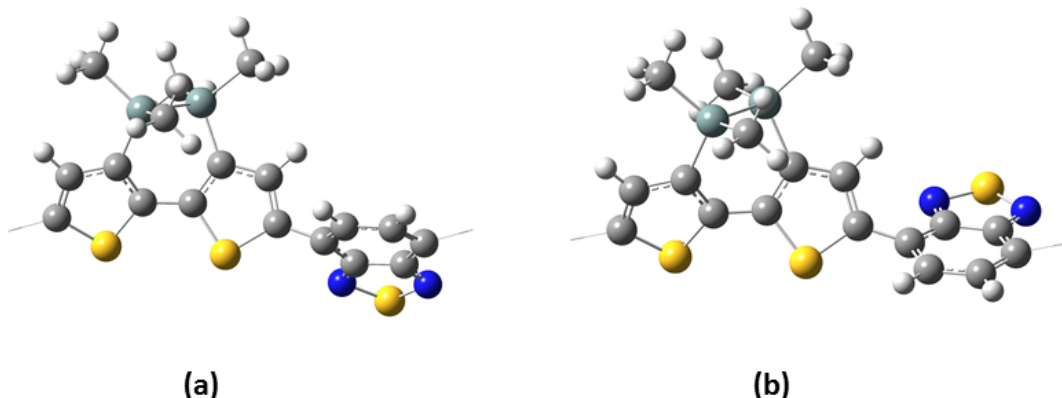


Figure S-3. Two kinds of plausible polymer structures of **pDSBT-BT** (shown by their unit cells) each of which has energetically local minimum. In these two, the structure (a) is the more stable than (b) by 1.19 kcal/mol per unit cell. Hence the conformation (a) is regarded as the unit cell of **pDSBT-BT** throughout this article.

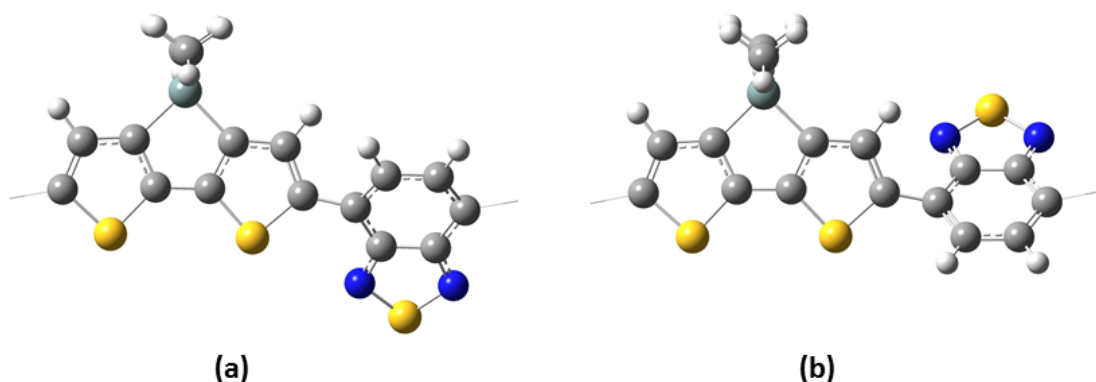


Figure S-4. Two kinds of plausible polymer structures of **pDTS-BT** (shown in their unit cells) each of which has energetically local minimum. In these two, the structure (a) is the more stable than (b) by 4.06 kcal/mol per unit cell. Hence the conformation (a) is regarded as the unit cell of **pDTS-BT** throughout this article.

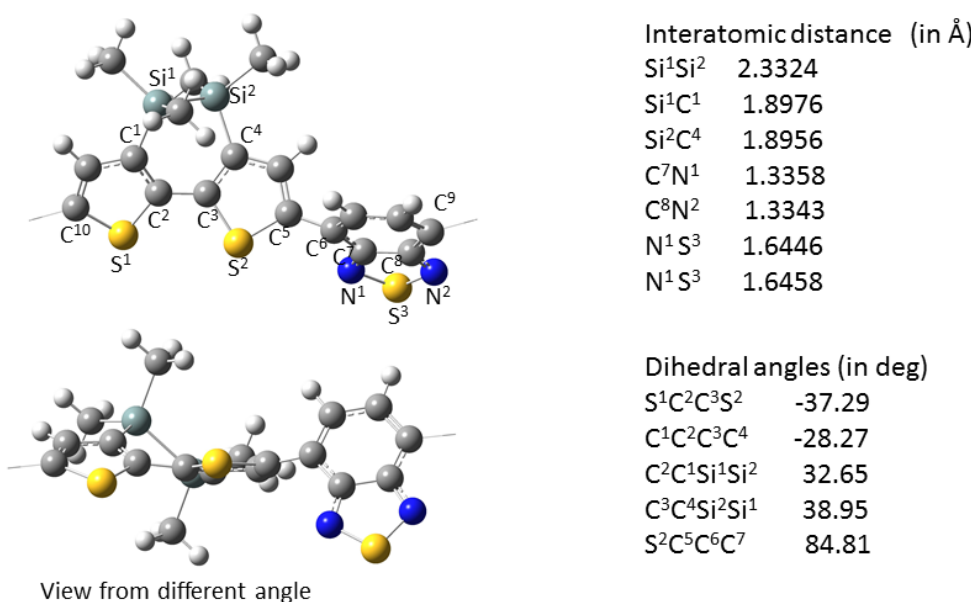


Figure S-5. Optimized structure of pDSBT-BT represented by its unit cell with selected bond lengths and dihedral angles. Note that the dihedral angles inside the bithiophene ring and between the thiophene and phenyl rings are 37.29 and 84.81 degrees, respectively, indicating larger off-planarity compared with that of pDTS-BT (see Figure S-6).

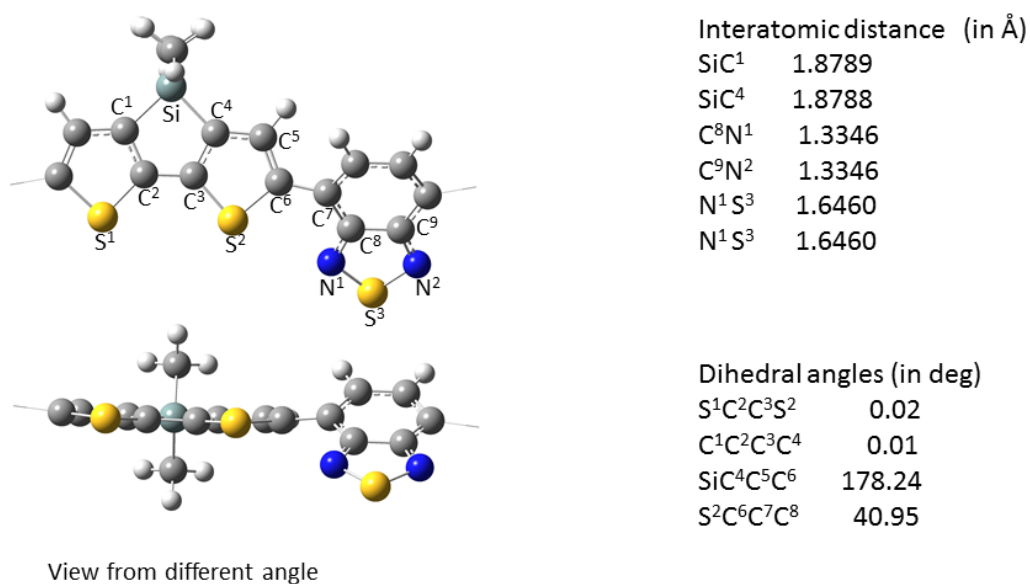


Figure S-6. Optimized structure of pDTS-BT represented by its unit cell with selected bond lengths and dihedral angles. Note that the dihedral angles inside the bithiophene ring and between the thiophene and phenyl rings are 0.02 and 40.95 degrees, respectively.

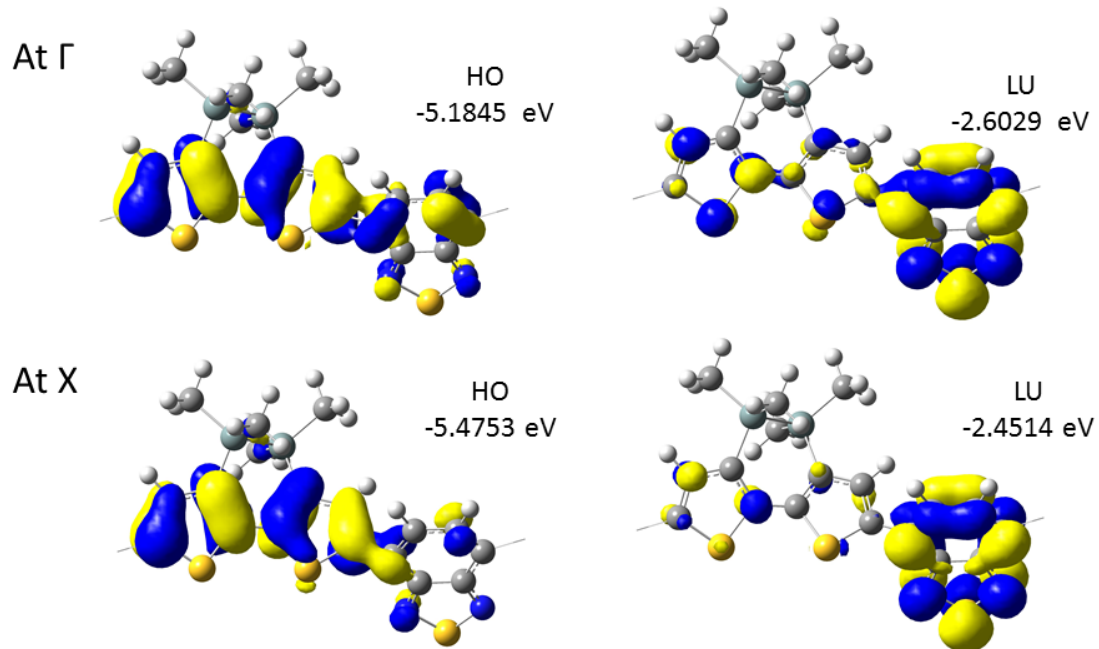


Figure S-7. The HOCO and the LUCO patterns with the orbital energies of pDSBT-BT represented on its unit cell at the Γ and the X points of the Brillouin zone. Note that the real HOCO and the LUCO are at the Γ point judging from their energy values.

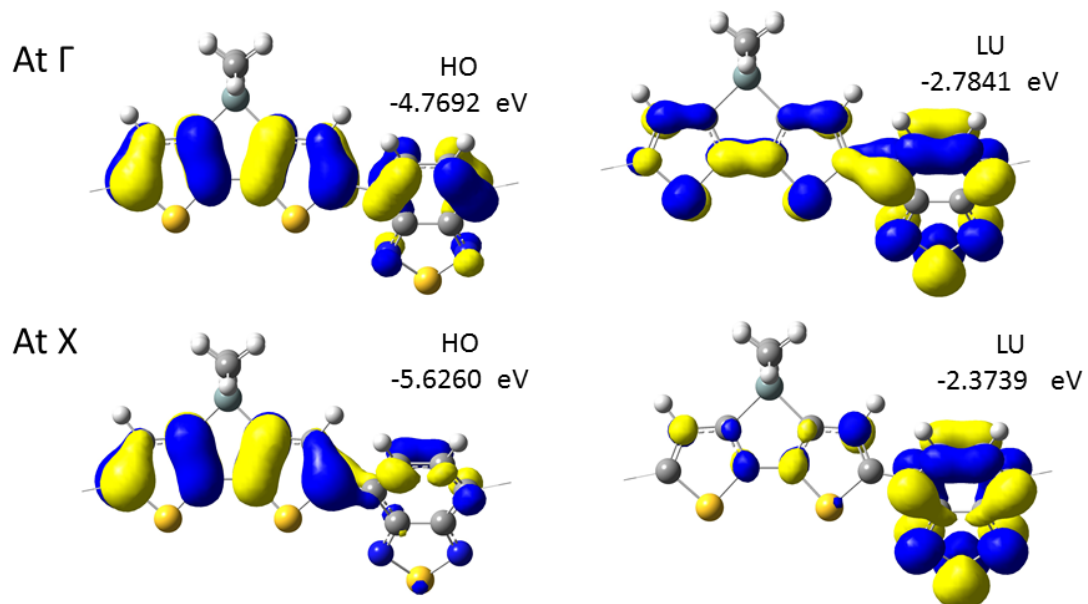


Figure S-8. The HOCO and the LUCO patterns with the orbital energies of pDTS-BT represented on its unit cell at the Γ and the X points of the Brillouin zone. Note that the real HOCO and the LUCO are at the Γ point judging from their energy values.

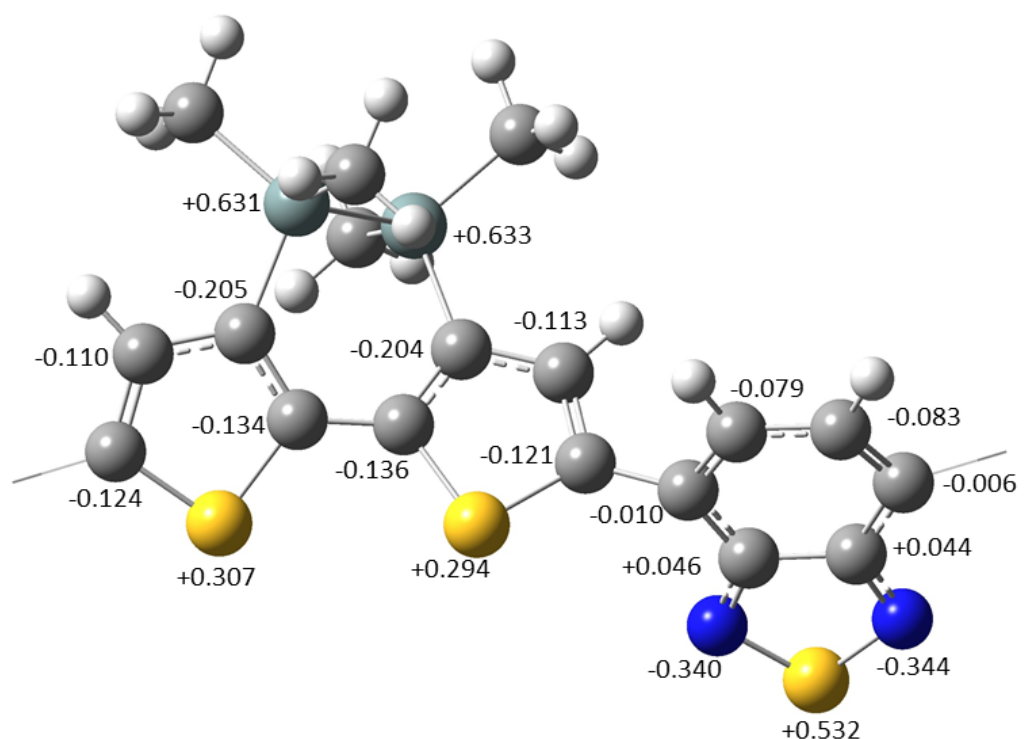


Figure S-9. Mulliken atomic net charges of pDSBT-BT.

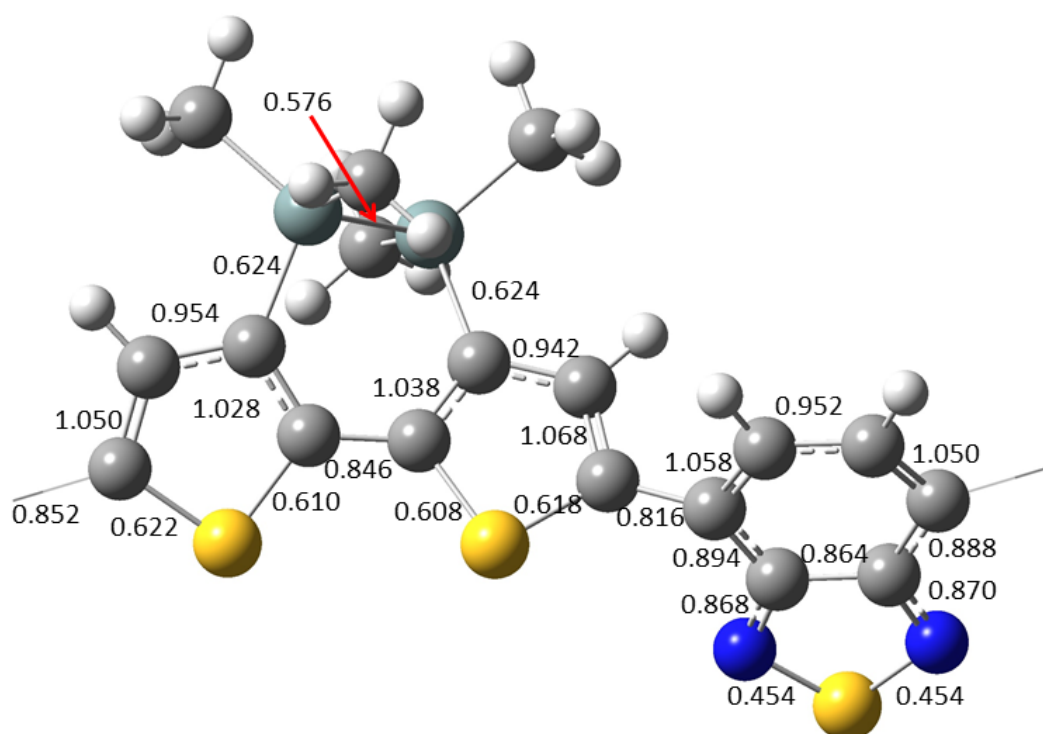


Figure S-10. Mulliken bond populations of pDSBT-BT.

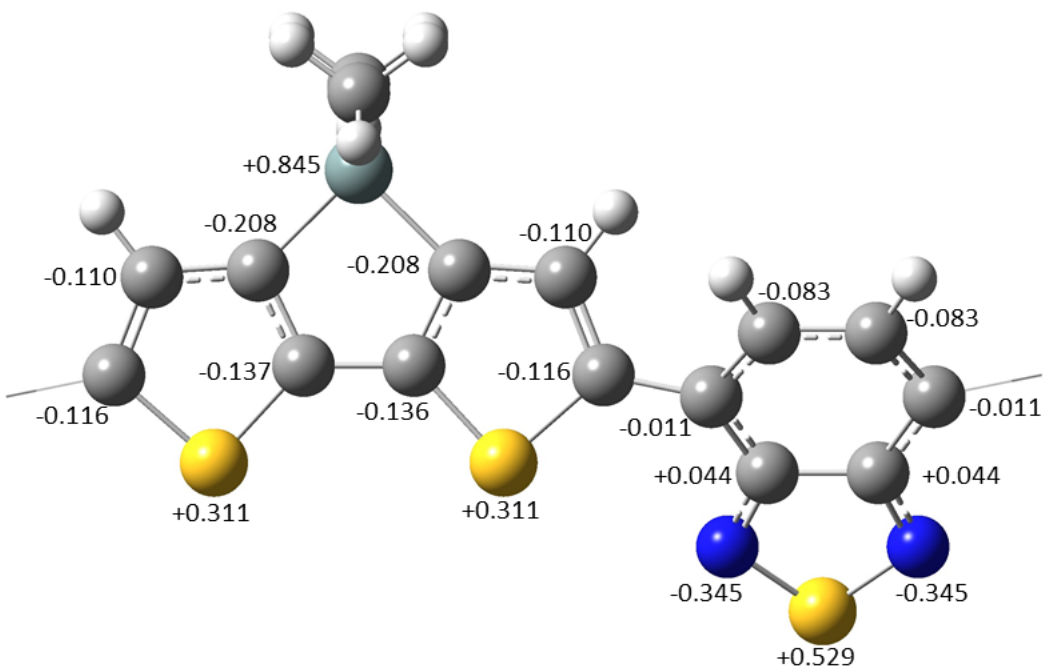


Figure S-11. Mulliken atomic net charges of pDTS-BT.

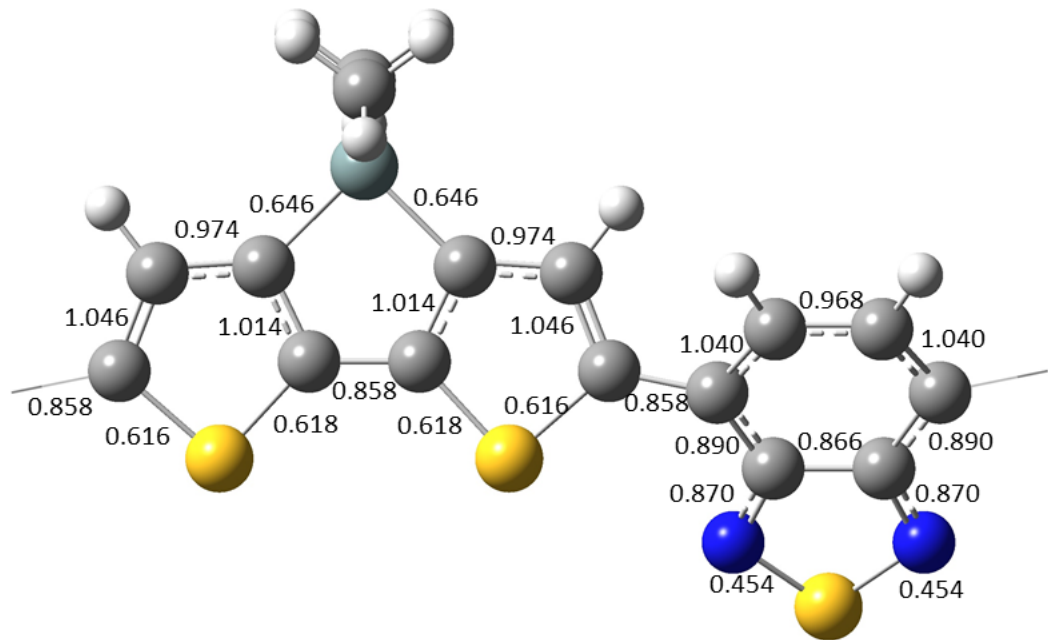


Figure S-12. Mulliken bond populations of pDTS-BT.